Graphical Abstract

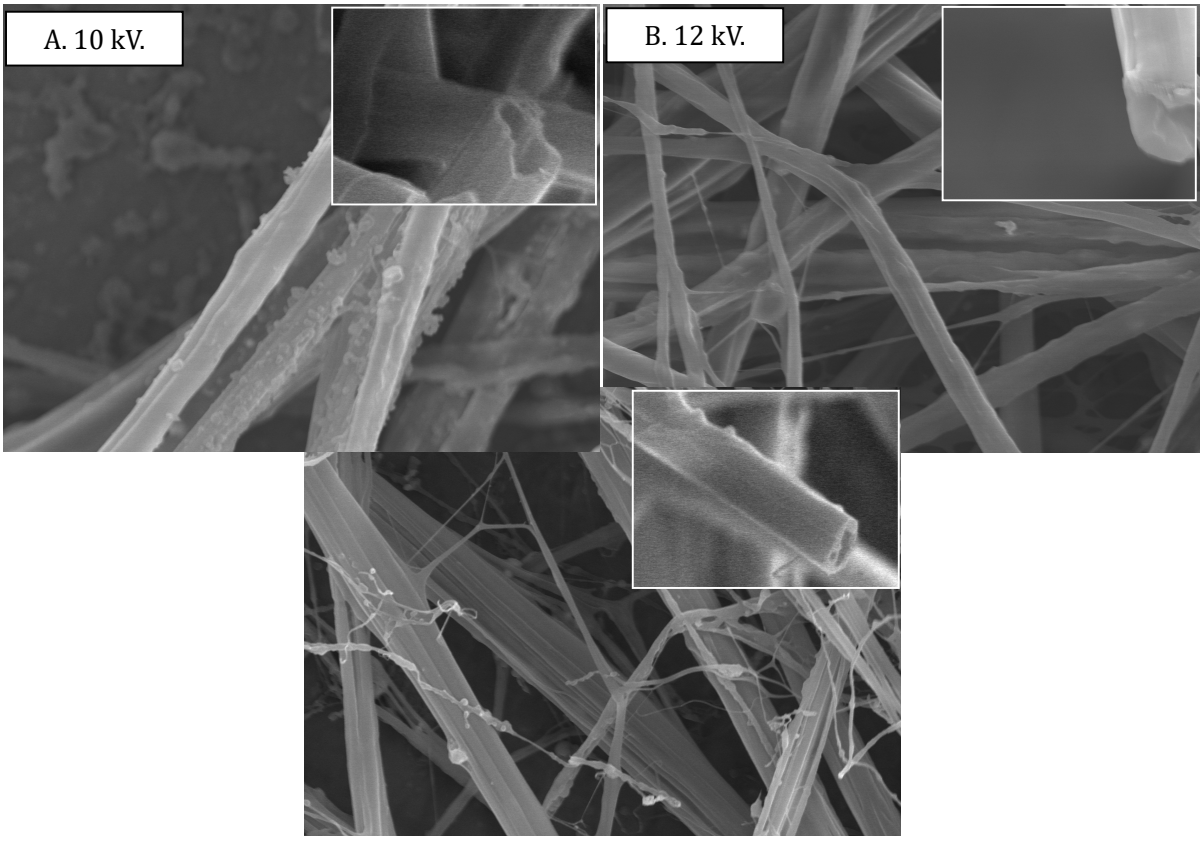

SEM images of PVP electrospun products with 25 nm TiO_2 nanoparticles at 5 MPa at various applied voltages, hollow fibers morphologies were formed.

Production of Poly(Vinyl Pyrrolidone) Fibers Containing Metal Oxides Nanoparticles by Electrospinning under Dense Carbon

Hiroyuki Ozawa[1], Siti Machmudah[2], Wahyudiono[3], Hideki Kanda[3], and Motonobu Goto[3,*]

[1]Department of Chemical Engineering, Nagoya University, Nagoya, 464–8603, Japan

[2]Department of Chemical Engineering, Sepuluh Nopember Institute of Technology, Surabaya 60111, Indonesia

[3]Department of Materials Process Engineering, Nagoya University, Nagoya, 464–8603, Japan

*Corresponding Author:

Email: goto.motonobu@material.nagoya-u.ac.jp; Tel.: +81–52–789–3992; Fax: +81–52–789–3989

Abstract

Electrospinning is known as a process of electrostatic fiber formation using electrical forces to produce polymer fibers in nano/micrometer scale diameters from polymer solution. In this study, poly(vinyl pyrrolidone) (PVP) dissolved in dichloromethane (DCM) with 4 wt% of concentration containing titanium oxide (TiO_2) nanoparticles was used as a polymer feed solution and is fed to electrospinning system under pressurized carbon dioxide (CO_2). The experiments are performed at temperature and pressure of 30 ^oC and 5 MPa with 10 – 14 kV applied voltages. The SEM images show that the PVP electrospun fibers products with and without TiO_2 nanoparticles have the same morphologies in hollow structures with average pores diameter 2 – 7 μm. The FT–IR spectra describes that the PVP electrospun fibers products seem to have similar properties of PVP starting material. The XPS spectra shows that the TiO_2 nanoparticles are found in the thermal gravimetric (TG) analysis residue of electrospun fibers products.

Keywords: Electrospinning, Hollow fibers, Dense CO_2, TiO_2, Poly(vinylpyrrolidone).

1. Introduction

Electrospinning has been known as a quite simple and versatile technique to produce polymer fibers in nano–micro scale from polymer solution. This technique has gained much attention due to its capability and feasibility to fabricate fibers in large quantities [1,2]. Hence, via this process, the production of nanofibrous mats or scaffolds can be realized. In a typical electrospinning apparatus, a syringe pump distributes a polymer solution through a spinneret into a high voltage electric field generated between the spinneret and a grounded collector. Therefore, it could be said that the driving force of elctrospinning process is electrostatic repulsion rather than a mechanical force. Compared with other techniques for nano–micro fibers production (e.g., drawing, template synthesis, phase separation, self–assembly), the electrospinning technique is the most efficient techniques for the realization of polymers fibers networks. This technique has also been applied to prepare metals, ceramics, and their composites, nanofiber structures with a large surface area, a high degree of porosity, and controlled surface functionalities [3,4].

In this work, ceramic nano–micro fibers were produced from PVP solution containing TiO_2 (titanium dioxide) by electrospinning under pressurized CO_2. PVP shows unique properties, including solubility in water or in organic solvent. Because PVP has low toxicity, high complexing ability, good film forming characteristics and adhesive properties, it was widely applied as excipients and is particularly suited to the preparation of solid dispersions for improving the dissolution rates of poorly water–soluble drugs in traditional pharmaceutical technologies [5–7]. Titanium and its alloys are common metallic biomaterials used for structural applications such as implants, pins, and bone scaffolding due to their excellent mechanical properties [8,9]. Titanium and titanium alloys have outstanding properties, including high biocompatibility, excellent corrosion resistance, resistance to body fluid effects, great tensile strength, and flexibility. They also show a unique combination of

strength and biocompatibility which enables their application in medical field (light, strong and totally biocompatible). Hence, titanium is one of the few materials that present a mechanical behavior close to those of bones and naturally match the requirements for implantation in the human body.

Here, PVP dissolved in dichloromethane (DCM) containing TiO_2 was directly introduced into electrospinning apparatus under dense CO_2 to produce nano–micro fibers. It has been known that CO_2 under dense conditions is a very poor solvent for virtually polymers and has poor reactivity towards the functional groups present in the polymers including PVP [10–12]. On the contrary, CO_2 at the same conditions may dissolve most organic solvents, such as acids, alcohols, and other low volatility solvents. Tsivintzelis et al. [13] reported phase compositions for the system CO_2–DCM at various temperatures and pressures. They informed that CO_2 seems having sufficient ability to bring a portion of the DCM. Due to these phenomena, our group have successfully produced hollow fibers from polymers in nano–micro scale with DCM as a polymer solvent in one step process [1,14–16]. The most of hollow fibers are fabricated by template–assisted techniques or by using a coaxial capillary. By using the selective dissolution or thermal degradation, the core of the electrospun fibers was removed to result hollow fibers. However, nano–micro fibers with hollow morphologies could be generated by simple depressurization at the end of the experiments when the electrospinning process were performed under dense CO_2 [17].

2. Experimental

2.1 Materials

PVP (MW 1,300,000) was purchased from Sigma–Aldrich and used as received. As a solution solvent, DCM (99.0%) was obtained from Wako Pure Chemical Industries, and was used without further purification. TiO_2 (25 and 100 nm) nanoparticles was purchased from

Wako Pure Chemical Industries and Sigma–Aldrich, respectively. Based on the previous researcher's reports [1,14–16], the 4 wt% concentration of PVP in DCM was chosen and used as a polymer feed solution. As a feed solution of electrospinning experiments, the small amount of TiO_2 was added in the polymer feed solution. So that, the feed solution was composed of a 10:1 weight ratio of polymer and TiO_2. Carbon dioxide (CO_2: 99%) was supplied by Sogo Kariya Sanso, Inc. Japan.

2.2 Experimental setup and methods

Fig. 1 describes the electrospinning apparatus under dense CO_2. The main apparatus composed of a nonconductive PEEK autoclave (AKICO PEEK), a high voltage (HV) power supply (Matsusada Precision HARb–30P1), a high pressure pump (JASCO PU–1586), a high pressure syringe pump (Harvard Apparatus PHD–Ultra 4400), a back–pressure regulator (BPR; AKICO HPB–450 SUS–316), and a stainless steel syringe. The nozzle–to–collector distance was 8 cm. In brief, the electrospinning experiment was conducted as follows. Initially, a nonconductive PEEK vessel was heated to a desired temperature of 30 ºC. After the desired temperature was achieved, CO_2 was introduced into the PEEK vessel via PEEK capillary tube to a desired pressure (5 MPa). This condition was selected based on the previous researcher's reports [1,14–16]. A BPR was employed to keep a constant pressure. When the desired condition was achieved, the feed solution was introduced into PEEK vessel by using high pressure stainless steel syringe placed in the high pressure syringe pump through PEEK capillary tube. The flow rate of feed solution was 0.05 mL min^{-1}. Next, the high voltage power supply was applied to generate electrostatic force. The experiment time was 15 min. In order to provide more reliable results, each experiment was conducted two to four times.

2.3 Fibers characterization

The morphologies of the electrospun fibers products were observed using a scanning electron microscope (SEM; Hitachi, S–4300, Japan) after gold coating (IB–3, Eiko

Engineering, Japan). The fiber diameter was measured from the SEM image using image analyzer software (Image J 1.42). The electrospun fibers products at each operating condition were analyzed using a Spectrum Two FT–IR spectrophotometer (PerkinElmer Ltd., England) to confirm the functional group of fibers. The spectra were measured in attenuated total reflectance (ATR) mode (golden single reflection ATR system, P/N 10500 series, Specac) at 4 cm^{-1} resolution. The scanning wave number ranged from 4000 to 400 cm^{-1}. The thermo–gravimetric/differential thermal analysis (TG 8120; Thermo plus, Rigaku, Corp., Japan) was also conducted to investigate the thermal behavior of electrospun fibers products. The XPS analysis was performed using an ESCA–3300 (Shimadzu–Kratos, Kyoto, Japan) with a collection angle of 45° from the normal to characterize surface of electrospun fibers products.

3. Results and Discussion

Fig. 2 shows SEM images of the PVP electrospun fibers products with and without TiO_2 nanoparticles under pressurized CO_2. In principle, electrospinning fabricates fibers with diameters ranging from nano– to micrometer scale when the electrostatic force is introduced on the polymer solutions. As informed before, the basic setup of electrospinning comprises three major components: a high–voltage power supply, a syringe with a metallic needle, and a grounded collector. When the high voltage was applied on the polymer solution which host by syringe via metallic needle, the drop of polymer solution at the metallic needle of syringe will be polarized and the induced charges will distribute on the polymer solution surface. Next, this applied voltage may cause a cone–shaped deformation of the drop of polymer solution. Once the power force of electric field was over than a threshold value, the electrostatic force on the drop of deformed polymer solution can overcome the surface tension of solvent and thus a liquid jet is generated. This electrified jet travels toward collector as a counter electrode, leading to the fibers formation. During travelling time, the polymer solvent is evaporated and

solid fibers were deposited on the fibers collector. Wahyudiono et al. [1] informed that one of the important features in electrospinning process was solvent evaporation. They informed that CO_2 may assist the evaporation process of polymer solvent due to its solubility in CO_2 by simple depressurization at the end of experiment. As shown in the Fig. 2, the PVP electrospun fibers products with and without TiO_2 nanoparticles seem dry and there was no remaining polymer solvent. These results indicated that CO_2 may promote the evaporation rate process of polymer solvent when it was used as an anti–solvent in electrospinning process. CO_2 will diffuse quickly into the polymer–solvent liquid jet and extract it. As a result, the nascent of PVP electrospun fibers products with and without TiO_2 nanoparticles are obtained in dry conditions [1,16].

Fig. 2 also shows that PVP electrospun fibers products with and without TiO_2 nanoparticles have hollow morphologies. The mechanism of these hollow fibers formation with and without TiO_2 nanoparticles are as follows: at first, the interaction between CO_2 and the PVP–DCM solution with and without containing TiO_2 nanoparticles at these conditions may promote the quick evaporation of polymer solvent (DCM) followed by the generation of phase boundaries and finally the PVP electrospun fibers products. CO_2 has been known as a very poor solvent to dissolve most polymers including PVP polymer even under supercritical conditions, conversely, at the same conditions, CO_2 may dissolve most organic solvents including DCM [11,12]. Since CO_2 may dissolve in DCM as a PVP solvent, the excess amounts of CO_2 might also dissolve into the DCM–rich liquid phase of polymer feed solution with and without containing TiO_2 nanoparticles. Next, the spinodal decomposition of PVP–DCM solution occurs to generate a network of PVP–DCM solution accompanied with CO_2–rich bubbles. Due to the coalescence and the expansion of the CO_2–rich bubbles in the PVP–DCM solution jet against the PVP–rich network occur continuously and the bubbles drive the PVP–rich phase radially outward against the inner surface of the jet, the PVP electrospun

fibers products with and without TiO_2 nanoparticles with hollow core can be generated [1,16]. In brief, Wahyudiono et al. [1,16] informed that the hollow fiber polymers could be generated by the outer fiber skin formation in first after polymer solvent was removed from the polymer nascent surface fiber. At the same time, CO_2 will also replace polymer solvent and promote the polymer swelling. Next, the hollow fibers morphologies were obtained when the CO_2 was removed from electrospun polymer products by simple depressurization at the end of experiment. Cooper [18,19] also informed that polymer micro-spheres and micro-balloons morphologies with hollow structures were found when polymer solution was sprayed and introduced to CO_2 vapor through a capillary tube. He explained that the hollow structures morphologies of them were formed due to the quick of drying and vitrification processes.

The SEM images of PVP electrospun fibers products with and without TiO_2 nanoparticles shown in Fig. 2 clearly depicted that there was no correlation significantly between the TiO_2 particles size added and the average fiber diameter generated in the electrospinning process. However, the broader range of fiber diameter was found when the TiO_2 nanoparticles were added in PVP solution used as a feed solution. From each image shown in Fig. 2, at least 300 different fibers were randomly selected, and their size were measured by using the Image J 1.42 tool to generate the fiber diameter distribution. Fig. 3 shows the fiber diameter distribution of PVP electrospun fibers products with and without TiO_2 nanoparticles. The average fiber diameter of PVP electrospun fibers products without TiO_2 nanoparticles was 2.64 ± 1.21 μm, and the average fiber diameter of them increased to 2.84 ± 1.99 and 2.67 ± 1.28 μm when TiO_2 nanoparticles with diameter 25 and 100 nm were added into PVP feed solution, respectively. Since the electrospinning process involves stretching of the polymer solution induced by repulsion of the charges at its surface, the polymer solution parameters had high effect on the conversion of polymer solutions into fibers during the electrospinning process [20,21]. As one of the polymer solution parameters,

the conductivity of polymer solution may affect on the charges that can be carried by the electrospinning jet. It can be improved by the addition of TiO_2 nanoparticles as ions sources [22,23]. It should be noted that the polymer feed solution conductivity was not measured during the course of an experiment. Nezarati et al. [21] reported that the increasing solution conductivity via the addition of salt can result in defect–free fibers and smaller diameter fibers. Li et al. [23] confirmed that the addition of tetrabutylammonium bromide on the polystyrene solution significantly improved the electrospinning process. They informed that the electrospun morphology changed from bead on–string structure to continuous and homogeneous fiber structure and leading to a smaller fiber diameter and narrower fiber diameter distribution. However, as shown in the Fig. 3, the addition of TiO_2 nanoparticles on the PVP feed solution seems no effect on the diameter of PVP electrospun fibers products. It could be explained that the effect of TiO_2 nanoparticles addition might vary from system to system [24]. Dersch et al. [25] predicted that the final electrospun fibers products diameter depends on the solution conductivity and varies as the cube root of the resistivity. But they also explained that only droplets were formed if the feed solution conductivity is very high and no continuous spinning could be reached if the feed solution conductivity is very low. In this case, the feed solution flow rate in the electrospinning system might be too small. Qin et al. [26] carried out experiments to study the effect of different salts on the electrospinning of polyacrylonitrile polymer solution. They informed that the higher conductivity of polyacrylonitrile polymer solution led to increase the mass flow dramatically during electrospinning process. As a result, the electrospun fibers products with the larger fiber diameters were formed dominantly. This is a main reason why the diameter of PVP electrospun fibers products seem to have a several micrometers scale in this work.

Fig. 4 shows the FT–IR spectrum of PVP electrospun fibers products with and without TiO_2 nanoparticles. This analysis is a powerful technique to identify a functional group. The

IR radiation beam able to penetrate the layer the sample surface and the penetration depth can be tuned within some range by selecting an appropriate prism. Hence, FT–IR can be applied to observe the possibility of PVP molecules structural change and to further obtain information on the interaction between PVP and titanium ions after electrospinning process. As a reference, the peak positions of all infrared bands and their functional groups are summarized in Table 1. Essentially, the FT–IR spectral characteristics of PVP and its electrospun fibers products with and without TiO_2 nanoparticles are the same, indicating that the electrospun products generated by electrospinning process are within a similar functional group as PVP [14]. This result also indicated that PVP is a good polymer substrate which employed in composite nano–micro fibers mats. Nevertheless, the peaks intensities in (b, c, and d) were sharper than (a) at 1651.12 – 1650.46 cm^{-1} region, describing that there was interaction between carbonyl bond in PVP with CO_2 molecules during electrospinning process. Perhaps, CO_2 molecules impregnated intensively to PVP. Hence, the H–bonding between PVP and CO_2 molecules are superior than interaction between DCM with the carbonyl groups of PVP [14]. Simultaneously, the strong interactions between the surface hydroxyl groups in the TiO_2 and hydrogen bonding in the PVP might also be occurred [27]. However, FT–IR is failure analysis on a variety of materials including metals, powdered metals, ores, ferroalloys, composites and ceramics [28]. Based on these results, it could be said that PVP electrospun fibers products with and without TiO_2 nanoparticles seem to have similar properties of PVP as a starting material. Due to FT–IR was not sufficient to observe the existence of TiO_2 nanoparticles in electrospun fibers products, other characterization techniques such as TG and XPS would be performed.

Fig. 5 shows the TG curves of PVP electrospun fibers products with and without TiO_2 nanoparticles. TG analysis is an analytical technique used to specify material's thermal stability and its fraction of volatile components by observing the weight change as a function

of increasing temperature with constant heating rate. This behavior has been clarified on the basis of heat transfer and medium diffusion [29,30]. The analysis was performed with a heating rate of 10 ºC min^{-1} using air flow (100 mL min^{-1}). The PVP electrospun fibers products with and without TiO_2 nanoparticles were weighed (approximately 0.5 – 1 mg) in open aluminum pans and the weight loss of them were monitored from 20 to 700 ºC. The weight loss was assumed to represent the thermal degradation of PVP electrospun fibers products with and without TiO_2 nanoparticles. It can be seen that there are several stages of the weight loss profile of them during the TG analysis process. Initial weight losses took place at around 80 ºC because of the evolution of volatile matter from PVP electrospun fibers products with and without TiO_2 nanoparticles. This process was then followed by a period of relatively constant weight. It seems that thermal degradation of PVP electrospun fibers products with and without TiO_2 nanoparticles were started at around 280 ºC, and followed a major loss of weight when the main devolatilization occurs and seems complete at around 620 ºC. After which there is essentially no further loss of weight. Generally, the addition of nanoparticles into polymer matrix can enhance the thermal stability due to the incorporation of nanoparticles added into the polymer matrix [31]. TiO_2 nanoparticles may dispersed in the PVP matrix during the fast evaporation of polymer solvent, further, the strong interaction between PVP and TiO_2 nanoparticles was formed via hydrogen bonding which exist in PVP matrix. However, as shown in Fig. 5, the thermal degradation curves of PVP electrospun fibers products with and without TiO_2 nanoparticles did not show significant differences. It is evident that the addition of TiO_2 nanoparticles into PVP feed solution did not give an effect to change the nature of the thermal degradation process [32]. Haldorai et al. [32] informed that the agglomeration of nanoparticles addition in the polymer sample may take place during preparation of polymer composites. As a result, the thermal stability of the polymer composites did not change significantly due to the systems turn from nanostructure to

microstructure.

Fig. 5 also shows that the weight reduction of the specimens observed at temperatures over 620 ºC was attributed to the existence of TiO_2 nanoparticles. Hence, the residual weight that remained is thought to be the weight of TiO_2 nanoparticles. This is, of course, a positive effect in terms of removing the polymer from the metal nanoparticles when the specimen would be analyzed by XPS. This analysis has been used to obtain detailed information on the chemical state of metals, e.g., TiO_2 nanoparticles. Here, XPS analysis was only employed to confirm the existence of TiO_2 nanoparticles in the TG analysis residue. In XPS analysis, the surface of specimen is exposed to monochromatic x–rays, whereby electrons are ejected due to the photoelectric effect. Therefore, the clear XPS spectra of the metal nanoparticles may not be found and observed when polymers cover the metal nanoparticles. Fig. 6 shows the XPS spectra of the TiO_2 nanoparticles obtained from the TG analysis residue of PVP electrospun fibers products containing TiO_2 nanoparticles with size 25 nm. PVP powder was used as a control. The peaks spectra at binding energies of 458 and 464 eV were detected clearly. It indicated that the existence of TiO_2 nanoparticles on the TG analysis residue was found [33]. Similar spectra was also obtained when the TG analysis residue of PVP electrospun fibers products containing TiO_2 nanoparticles with size 100 nm was submitted in the XPS apparatus [34]. Thus, the XPS data for TG residue of PVP electrospun fibers products containing TiO_2 nanoparticles with size 100 nm was not presented. Zhang et al. [34] conducted experiments to examine whether the oxidation state of surface Ti atoms are the same for three different TiO_2 nanoparticles with different sizes. The same XPS spectra for TiO_2 nanoparticles with various particles size were found. They concluded that the shapes of the Ti 2p doublet are virtually the same for all samples size which results Ti^{4+} as oxidation state of the surface Ti atoms for the all samples size.

Fig. 7 shows SEM images of the PVP electrospun fibers products containing TiO_2

nanoparticles when the electrospinning process was performed at 10 to 14 kV applied voltages. In electrospinning process, the applied voltage may determine the strength of electrical field, which strongly influence the properties of polymer solution jet to generate electrospun fibers products. Therefore, the applied voltage plays a crucial role in the electrospinning process to control the morphologies of electrospun fibers products. When the applied voltage increases, there were two different effects on the fiber diameter could be found: stretching force on solution jet generally increases with the increasing applied voltage to generate the finer fibers. Second, the higher applied voltage favored to the formation of defects along the fibers, therefore the probability of bead formation increases as a higher voltage is applied if the polymer feed concentration was not sufficient [35]. It could be said that the effect of the applied voltage on the bead formation is not absolute, like many other electrospinning parameters. As shown in Fig. 7, no beads formation can be observed on all PVP electrospun fibers products containing TiO_2 nanoparticles. It indicated that the applied voltages employed to generate electric field is properly adjusted. The increasing applied voltages may increase the electrostatic repulsive force on the charged polymer solution jet and give influence on the stretching and acceleration of the jet thinning to electrospun fibers products collector. This might be the reason why the beads were not drawn and found on the electrospun fibers products collector. Meanwhile, as shown in Fig. 8, the electrospun fiber diameter distribution of PVP electrospun fibers products containing TiO_2 nanoparticles seems smaller with increasing the applied voltage. The applied voltage of 14 kV yielded electrospun fibers products with an average diameter of 2.84 $\pm$ 1.99 μm, while the electrospun fibers products with an average diameter of 7.48 $\pm$ 3.65 μm were obtained when the applied voltage of electrospinning was 10 kV. Again, it showed that the electrostatic forces which acts on the polymer feed droplet increased due to the increasing applied voltage. The increasing applied voltage may provide an additional force to overcome viscoelastic and surface tension forces

exerted by the polymer feed solution. Next, the increasing applied voltage will promote the elongation of the polymer solution jet and lead to finer fibers [36].

4. **Conclusions**

The production of PVP fibers with and without TiO_2 nanoparticles by electrospinning at 10 – 14 kV was studied at a temperature and pressure of 30 ºC and 5 MPa, respectively. The SEM images described that the PVP electrospun fibers products with and without TiO_2 nanoparticles have the same morphologies. They seem to have hollow morphologies. The FT–IR spectra showed that the PVP electrospun fibers products with and without TiO_2 nanoparticles seem to have similar properties of PVP as a starting material. The XPS spectra gave an information that the TiO_2 nanoparticles were found in the TG analysis residue of electrospun fibers products. The fiber diameter of electrospun fibers products seems smaller with increasing the applied voltage without bead formation. This work demonstrated that this process is new and offers the possibility that electrospinning under pressurized CO_2 will become an essential and useful technique for the fabrication of organic polymer structures with hollow interiors containing metal nanoparticles.

References

[1] Wahyudiono, S. Machmudah, H. Kanda, S. Okubayashi, M. Goto, Chem. Eng. Process. Process Intensif. **77**, 1 (2014).

[2] J. Quiros, K. Boltes, R. Rosal, Polym. Rev. **56**, 631 (2016).

[3] H. Wu, W. Pan, D. Lin, H. Li, J. Adv. Ceram. **1**, 2 (2012).

[4] X. Shi, W. Zhou, D. Ma, Q. Ma, D. Bridges, Y. Ma, A. Hu, J. Nanomater. **2015**, ID 140716 (2015) http://dx.doi.org/10.1155/2015/140716.

[5] G. Van den Mooter, P. Augustijns, N. Blaton, R. Kinget, Int. J. Pharm. 64, 67 (1998).

[6] C. Leuner, J. Dressman, Eur. J. Pharm. Biopharm. **50**, 47 (2000).

[7] G. Verreck, A. Decorte, K. Heymans, J. C. D. Adriaensen, A. Jacobs, D. Liu, D. Tomasko, A. Arien, J. Peeters, P. Rombaut, G. Van den Mooter, M. E. Brew-ster, Eur. J. Pharm. Sci. **26**, 349 (2005).

[8] M. Prakasam, J. Locs, K. Salma-Ancane, D. Loca, A. Largeteau, L. Berzina-Cimdina, J. Funct. Biomater. **6**, 1099 (2015).

[9] M. Kulkarni, A. Mazare, E. Gongadze, S. Perutkova, V. Kralj-Iglic, I. Milosev, P. Schmuki, A. Iglic, M. Mozeti, Nanotechnol. **26**, 062002 (2015) doi:10.1088/0957-4484/26/6/062002.

[10] C. F. Kirby, M. A. McHugh, Chem. Rev. **99**, 565 (1999).

[11] W. Bae, S. Kwon, H. S. Byun, H. Kim, J. Supercrit. Fluids **30**, 127 (2004).

[12] M. S. Shin, J. H. Lee, H. Kim, Fluid Phase Equilib. **272**, 42 (2008).

[13] I. Tsivintzelis, D. Missopolinou, K. Kalogiannis, C. Panayiotou, Fluid Phase Equilib. **224**, 89 (2004).

[14] Wahyudiono, K. Murakami, S. Machmudah, M. Sasaki, M. Goto, Jpn. J. Appl. Phys. **51**, 08HF07 (2012).

[15] Wahyudiono, S. Machmudah, K. Murakami, S. Okubayashi, M. Goto, IJIC **4**, 27 (2013) doi:10.1186/2228-5547-4-27.

[16] Wahyudiono, K. Okamoto, S. Machmudah, H. Kanda, M. Goto, Polym. Eng. Sci. **56**, 752 (2016).

[17] M. F. Kemmere, T. Meyer, Supercritical Carbon Dioxide in Polymer Reaction Engineering (Wiley-VCH Verlag GmbH & Co. KGaA, Weinheim, Germany 2005), pp. 260.

[18] A. I. Cooper, J. Mater. Chem. **10**, 207 (2000).

[19] A. I. Cooper, Adv. Mater. **15**, 1049 (2003).

[20] T. Liu, D. Lv, B. Cao, H. Wang, J. Appl. Polym. Sci. **126**, 1977 (2012).

[21] R. M. Nezarati, M. B. Eifert, E. Cosgriff-Hernandez, Tissue Eng. Part C Methods **19**, 810 (2013).

[22] G. Xiong, A. Kundu, T. S. Fisher, Thermal effects in supercapacitors (Springer International Publishing 2015), pp. 52.

[23] Y. Li, H. Porwal, Z. Huang, H. Zhang, E. Bilotti, T. Peijs, J. Nanomater. **2016**, 18, ID 4624976 (2016) http://dx.doi.org/10.1155/2016/4624976.

[24] S. Agarwal, M. Burgard, A. Greiner, J. Wendorff, Electrospinning: A Practical Guide to Nanofibers (Walter de Gruyter GmbH & Co KG 2016), pp. 108.

[25] R. Dersch, A. Greiner, J. H. Wendorff, Polymer nanofibers prepared by electrospinning (Dekker encyclopedia of nanoscience and nanotechnology, CRC, New York 2009), pp. 3480.

[26] X. H. Qin, E. L. Yang, N. Li, S. Y. Wang, J. Appl. Polym. Sci. **103**, 3865 (2007).

[27] G. S. Anjusree, A. Bhupathi, A. Balakrishnan, S. Vadukumpully, K. R. V. Subramanian, N. Sivakumar, S. Ramakrishna, S. V. Nair, A. S. Nair, RSC Adv. **3**, 16720 (2013).

[28] S. Thomas, Rheology and Processing of Polymer Nanocomposites (John Wiley & Sons 2016), pp. 335.

[29] P. T. Williams, S. Besler, Renewable Energy **7**, 233 (1996).

[30] A. Arenillas, F. Rubiera, J. Anal. Appl. Pyrolysis **58-59**, 685 (2001).

[31] K. Chrissafis, D. Bikiaris, Thermochim. Acta **523**, 1 (2011).

[32] Y. Haldorai, W. S. Lyoo, S. K. Noh, J. J. Shim, React. Funct. Polym. **70**, 393 (2010).

[33] L. B. Xiong, J. L. Li, B. Yang, Y. Yu, J. Nanomater. **2012**, 9, ID 831524 (2012) http://dx.doi.org/10.1155/2012/831524.

[34] Q. L. Zhang, L. C. Du, Y. X. Weng, L. Wang, H. Y. Chen, J. Q. Li, J. Phys. Chem. B **108**, 15077 (2004).

[35] Y. Liu, L. Dong, J. Fan, R. Wang, J. Y. Yu, J. Appl. Polym. Sci. **120**, 592 (2011).

[36] V. Pillay, C. Dott, Y. E. Choonara, C. Tyagi, L. Tomar, P. Kumar, L. C. du Toit, V. M. Ndesendo, J. Nanomater. **2013**, ID 789289 (2013) http://dx.doi.org/10.1155/2013/789289.

[37] **Table captions**

Table 1. Wave number assignments of FT–IR spectra.

Figure captions

Fig. 1. Apparatus scheme of the electrospinning system. (1. CO_2 cylinder; 2. Syringe; 3. Syringe pump; 4. CO_2 pump; 5. Nozzle; 6. Collector; 7. High voltage source; 8. Spinning–Autoclave; 9. Temperature sensor; 10. BPR; 11. Solvent trap; 12. Flow meter; 13. Heater).

Fig. 2. SEM images of PVP electrospun fibers products with and without TiO_2 nanoparticles at 5 MPa with 14 kV applied voltage: (A) PVP, (B) PVP + 25 nm TiO_2 nanoparticles, (C) PVP + 100 nm TiO_2 nanoparticles.

Fig. 3. The electrospun fiber diameter distribution of PVP electrospun fibers products with and without TiO_2 nanoparticles at 5 MPa with 14 kV applied voltage: (A) PVP, (B) PVP + 25 nm TiO_2 nanoparticles, (C) PVP + 100 nm TiO_2 nanoparticles.

Fig. 4. FT–IR spectrum of PVP raw material and its electrospun fibers products with and without TiO_2 nanoparticles at 5 MPa with 14 kV applied voltage: (A) PVP raw material, (B) PVP electrospun, (C) PVP + 25 nm TiO_2 nanoparticles, (D) PVP + 100 nm TiO_2 nanoparticles, respectively.

Fig. 5. TG curves of PVP electrospun fibers products with and without TiO_2 nanoparticles at 5 MPa with 14 kV applied voltage: (A) PVP, (B) PVP + 25 nm TiO_2 nanoparticles, (C) PVP + 100 nm TiO_2 nanoparticles, respectively.

Fig. 6. XPS spectra of PVP electrospun fibers products (A) with and (B) without TiO_2 nanoparticles at 5 MPa with 14 kV applied voltage.

Fig. 7. SEM images of PVP electrospun fibers products with 25 nm TiO_2 nanoparticles at 5 MPa at various applied voltages: (A) 10 kV, (B) 12 kV, (C) 14 kV.

Fig. 8. The electrospun fiber diameter distribution of PVP electrospun fibers products with TiO_2 nanoparticles at 5 MPa at various applied voltages: (A) 10 kV, (B) 12 kV, (C) 14 kV.

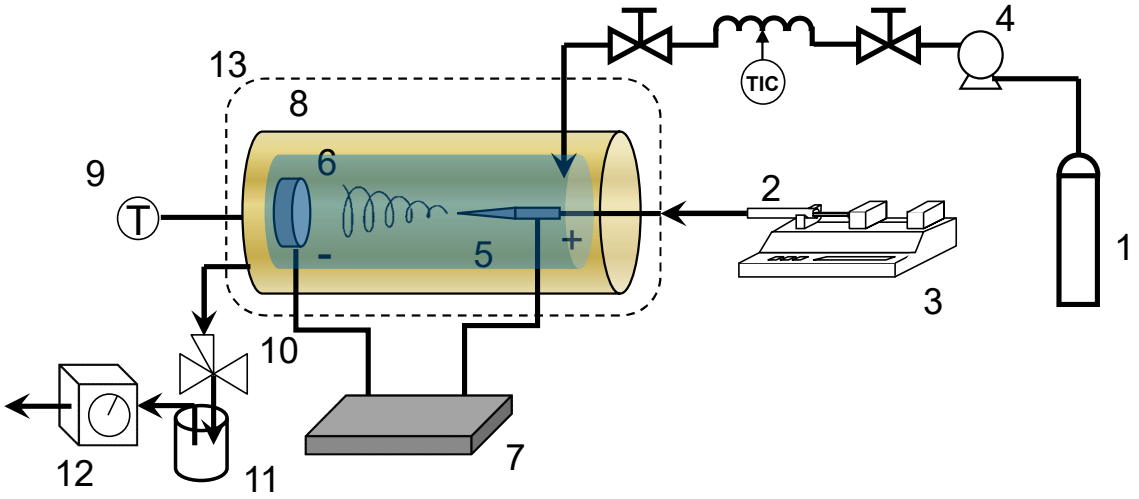

Figure 1

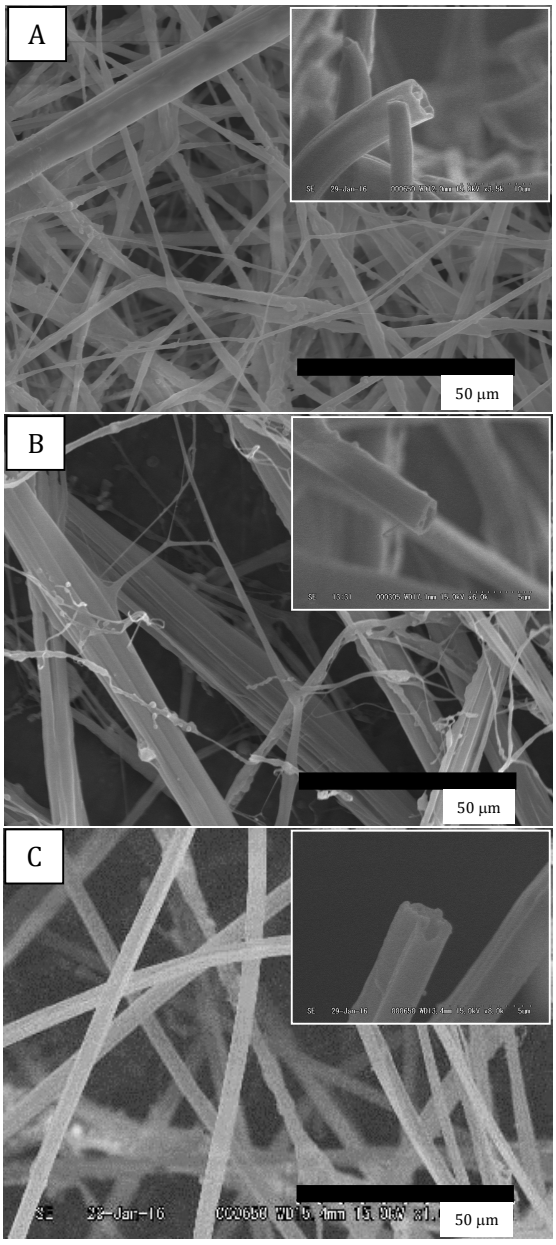

Figure 2

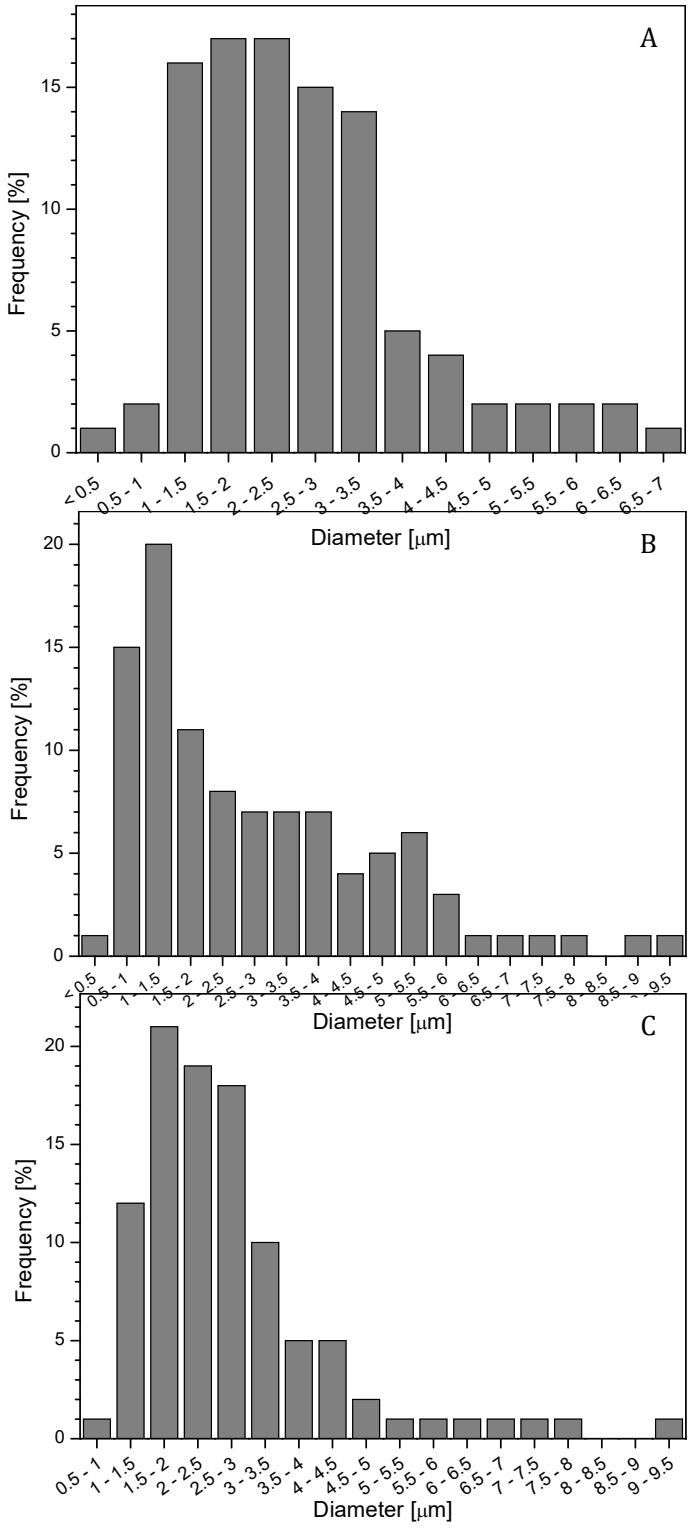
A
Frequency [%]
0
5
10
15
< 0.5
0.5 - 1
1 - 1.5
1.5 - 2
2 - 2.5
2.5 - 3
3 - 3.5
3.5 - 4
4 - 4.5
4.5 - 5
5 - 5.5
5.5 - 6
6 - 6.5
6.5 - 7
Diameter [μm]
B
Frequency [%]
0
5
10
15
20
< 0.5
0.5 - 1
1 - 1.5
1.5 - 2
2 - 2.5
2.5 - 3
3 - 3.5
3.5 - 4
4 - 4.5
4.5 - 5
5 - 5.5
5.5 - 6
6 - 6.5
6.5 - 7
7 - 7.5
7.5 - 8
8 - 8.5
8.5 - 9
9 - 9.5
Diameter [μm]
C
Frequency [%]
0
5
10
15
20
0.5 - 1
1 - 1.5
1.5 - 2
2 - 2.5
2.5 - 3
3 - 3.5
3.5 - 4
4 - 4.5
4.5 - 5
5 - 5.5
5.5 - 6
6 - 6.5
6.5 - 7
7 - 7.5
7.5 - 8
8 - 8.5
8.5 - 9
9 - 9.5
Diameter [μm]

Figure 3

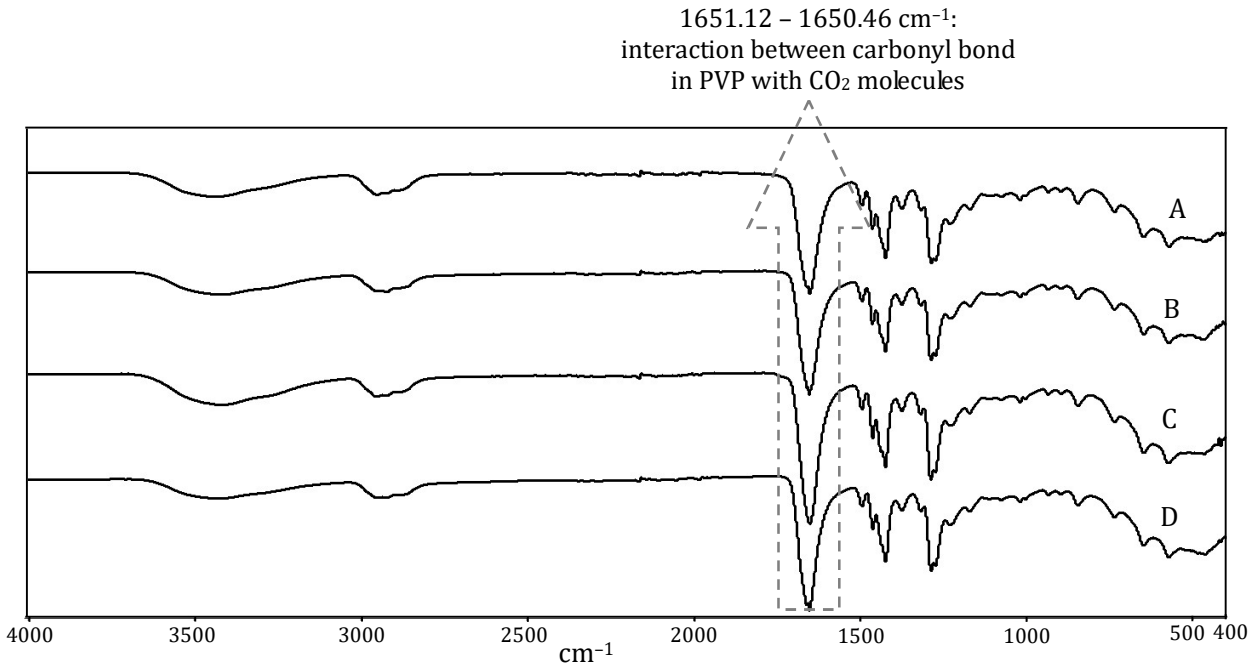
1651.12 – 1650.46 cm⁻¹:
interaction between carbonyl bond
in PVP with CO2 molecules
A
B
C
D
4000
3500
3000
2500
2000
1500
1000
500 400
cm⁻¹

Figure 4

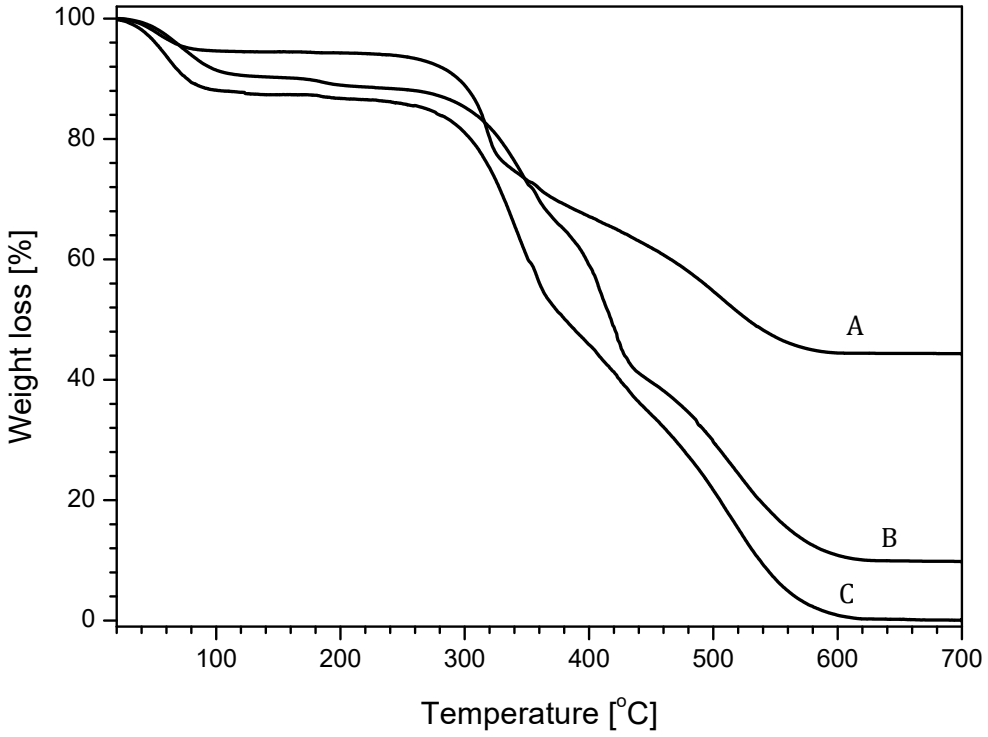
100
80
60
40
20
0
Weight loss [%]
100
200
300
400
500
600
700
Temperature [°C]
A
B
C

Figure 5

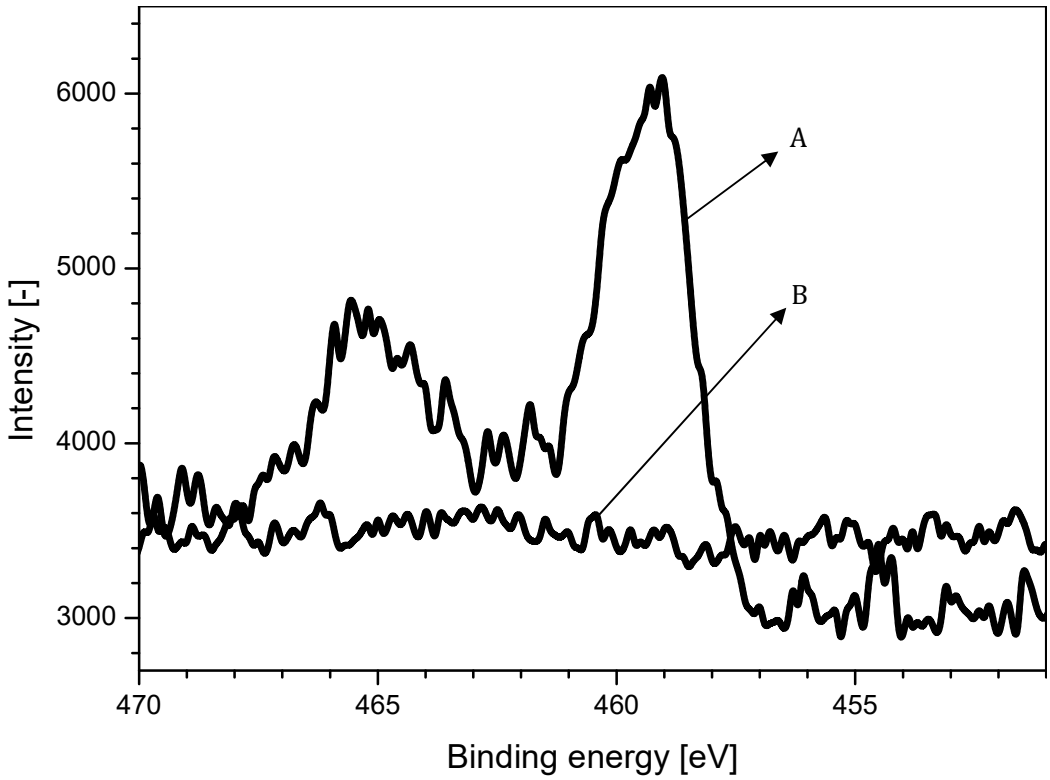
6000
5000
4000
3000
Intensity [-]
470
465
460
455
Binding energy [eV]
A
B

Figure 6

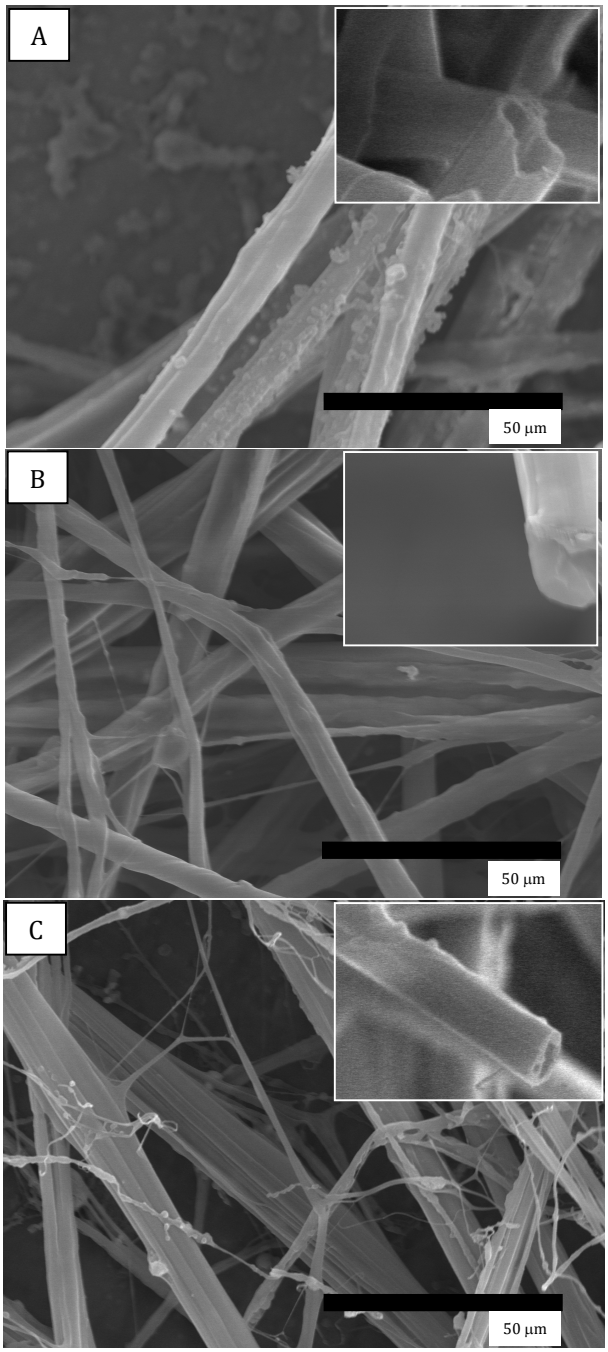

Figure 7

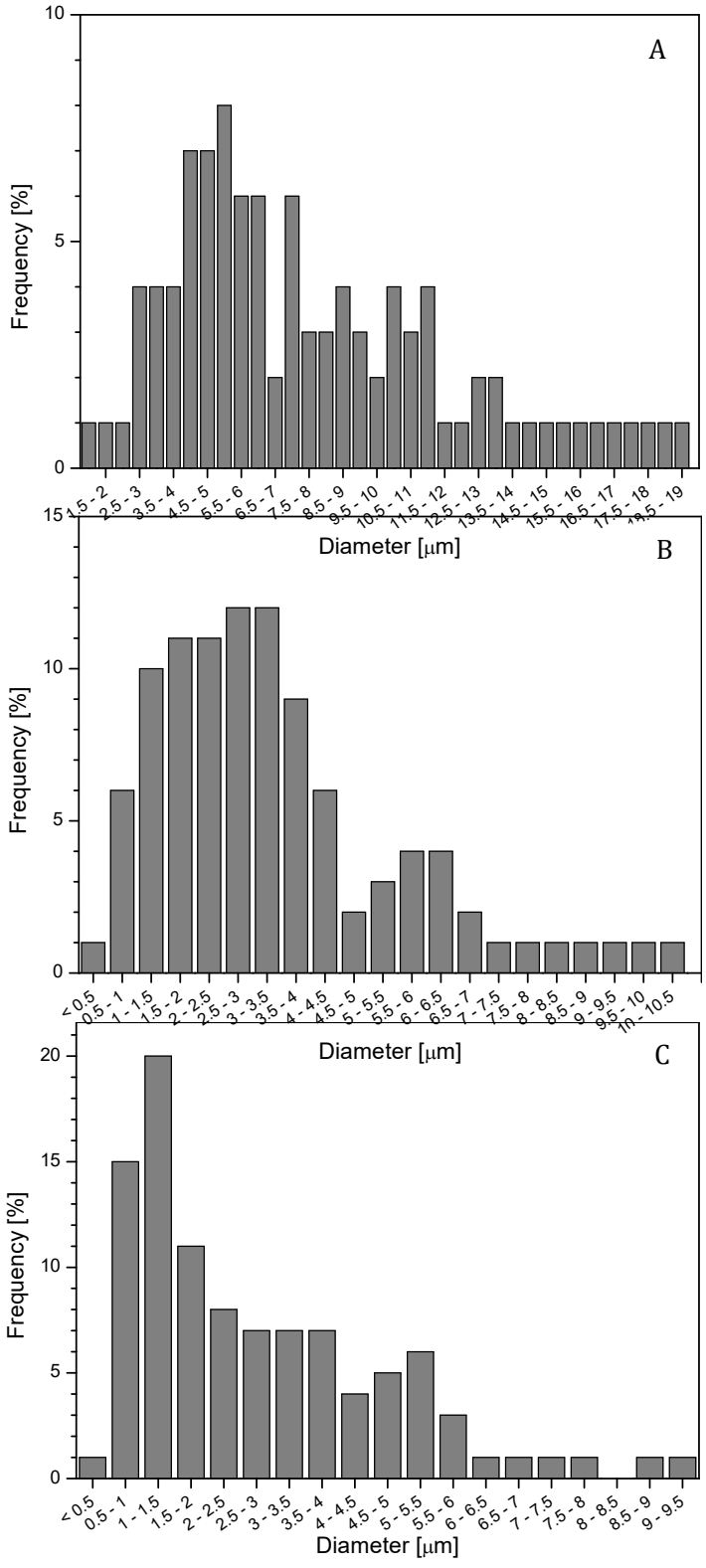
A
Frequency [%]
Diameter [μm]
B
Frequency [%]
Diameter [μm]
C
Frequency [%]
Diameter [μm]

Figure 8

Table 1

Wave number [cm^{-1}]	Functional groups
3435.47–3415.45 and 1286.37–1284.84	Related to N–H stretching vibration and C–N stretching vibration from pyrrolidone structure
2950.02–2921.18	Related to C–H stretching for aliphatic compounds
1651.12–1650.46	Associated to carbonyl (C–O) stretching of the five membered cyclic lactam structure
1493.25–1493.16 and 1461.00–1460.82	Related to C=C aromatic stretching
1422.11–1421.63 and 1372.91–1372.32	Attributed to C–H bending vibration from methylene groups (aliphatic compound)
843.82–843.29	Associated to =C–H bending vibrations (unsaturated compounds)